16th World Conference on Earthquake, 16WCEE 2017
Santiago Chile, January 9th to 13th 2017
Paper N° 196 (Abstract ID)
Registration Code: S-N1461219190

NUMERICAL MODELLING OF HEATING EFFECTS IN CURVED SURFACE SLIDING ISOLATORS

V. Quaglini[(1)], P. Dubini[(2)], E Gandelli[2)]

[(1)] *Associate Professor, Politecnico di Milano, Department of Architecture, Built Environment and Construction Engineering, virginio.quaglini@polimi.it*
[(2)] *Research Fellow, Politecnico di Milano, Department of Architecture, Built Environment and Construction Engineering, paolo.dubini@polimi.it*
[(3)] *PhD Candidate, Politecnico di Milano, Department of Architecture, Built Environment and Construction Engineering, emanuele.gandelli@polimi.it*

Abstract

The Curved Surface Slider, also known as the Friction Pendulum System, has become in the last years a very popular antiseismic hardware for base isolation of buildings and structures. A potential issue for sliding isolation systems is the degradation of the coefficient of friction caused by the temperature growth within the bearing due to the dissipation of the seismic energy as frictional heat. Both experimental and numerical investigations have pointed to the importance of the issue, and models accounting for the temperature dependence of the coefficient of friction at the material level have been recently proposed, which can be used in finite element analyses of the whole isolator.

In this study, a three-dimensional finite element model of a Curved Surface Slider unit developed by the Authors is used to investigate in detail the influence of the path of motion on the temperature growth. In the first part, the finite element formulation and its validation are presented. The generation of frictional heat is reproduced in the model by locating a heat source on the surface of the sliding pad, with intensity of the heat flux depending on the coefficient of friction, the axial pressure, and the velocity. The coefficient of friction at the material level is routinely adjusted by the software at each calculation step on the current levels of pressure, velocity and temperature. In the second part, either unidirectional and multidirectional displacement-controlled orbits are challenged in finite element thermal-mechanical analyses in order to investigate the temperature growth inside the bearing and the relevant changes in the mechanical response of the device. The result point to the unsuitability of the unidirectional trajectories performed in the tests prescribed in current standards to reproduce the temperature rises that may possibly occur within the Curved Surface Slider unit under more general multidirectional orbits typical of real earthquakes.

Keywords: frictional heating; curved surface slider; seismic isolation

1. Introduction

Among the most popular antiseismic hardware today, there is the Curved Surface Slider (CSS), introduced in the USA in the '80s of the last century in the version called the Friction Pendulum System® (FPS®) [1-3] and whose use has spread worldwide after the expiry of patent rights in 2005. Current standards in North America and in Europe regulate the design, manufacture and testing of the CSS [4-6]. However, a considerable progress has been made in the recent years towards a more detailed knowledge of the behavior of sliding isolators, which may create a gap between the available knowledge and the already established standards.

An issue that has come under the spotlight only in the last few years is the frictional heating [7-8]. The Curved Surface Slider dissipates the seismic energy by means of friction developed at the sliding surface, and the most of this frictional power is converted into heat. In presence of large friction forces and high speeds typical of strong earthquakes, the level of frictional heat can be very huge and produce an important growth of temperature at the surface. A first effect is that the temperature rise may accelerate wear and even promote failure of the surface liner material, which is usually made of PTFE [9] or UHMWPE [10]; a second effect is that the coefficient of friction of thermoplastic materials tends to decrease with an increase of temperature [9, 11], changing the mechanical properties of the isolation system. The first experimental studies pointing to thermal heating in sliding isolators were reported more than ten years ago [12, 13], but it was evident that due to the inherent complexity of the phenomenon and the large number of factors involved, laboratory experiments alone were not sufficient to assess the thermal response of CSSs under real earthquake attacks. Theoretical models and calculation procedures were then developed to assist the experimental investigation.

Constantinou [7] presented an analytical model to calculate the temperature rise in the Friction Pendulum System at both the sliding surface and at small depths below. For a large FPS bearing designed to carry a gravity load of more than 75 MN in an offshore platform [14] subjected to biaxial motion at velocities up to 0.8 m/s, peak temperatures as high as 400°C were predicted. Drozdov [15] performed a finite element investigation of the steady-state temperature in a spherical bearing under different loading parameters, concluding that estimating the temperature inside the FPS is a fundamental issue in order to choose suitable materials according to their temperature stability. These studies focused on the temperature growth within the bearing and did not take into account the effect on the coefficient of friction. Numerical analyses with consideration of the dependence of the friction on temperature were recently presented by Quaglini [8] and Kumar [16], demonstrating that ignoring the thermal contribution may considerably overestimate the isolator's damping capability during the seismic attack.

Current standards have indeed noted this issue and established prescriptions to limit the change of the dynamic properties of the isolator: according to the European standard EN 15129 [4], the maximum resisting force and the energy dissipated per cycle (EDC) measured in unidirectional tests shall deviate no more than 15% in three cycles of motion up to the design displacement. ASCE/SEI 7-10 [5] prescribes a maximum deviation of 20% over ten cycles of loading, while the AASHTO Specification [6] recommends after twenty cycles of loading a maximum variation of the effective stiffness and the EDC less than 20% and 30% respectively. The standards' prescriptions are based on unidirectional testing because they are simpler, less demanding and can be performed by a large number of facilities worldwide. However recent experience from bidirectional tests on full scale isolators [17-19] points to the fact that the temperature growth is influenced from the path of motion of the bearing, though the effect of prior heating of the surface during the passage of the slider. Therefore, the unidirectional periodic motion developed in the tests according to the standards may not be able to replicate with sufficient accuracy the actual heat-flux history and temperature rise occurring during the actual motion of a CSS in a real earthquake which in general follows a chaotic multidirectional orbit.

In this study, the influence of the orbit of displacement-controlled tests on the response of a Curved Surface Slider accounting for the effects of frictional heating is investigated by using the numerical procedure developed by Quaglini and co-workers [8]. The formulation of the finite element model and the validation of the procedure are briefly summarized in section 2. Unidirectional and multidirectional orbits are simulated and the CSS response calculated and assessed in terms of force and temperature histories. The discussion is focused on the accuracy of the unidirectional tests for evaluating the performances of the bearing under more general multidirectional trajectories.

2. Finite element formulation

2.1 C description

The CSS unit considered as case study is a conventional isolator provided with a primary surface that accommodates the horizontal displacement and a secondary surface that permits the rotation of the slider (Fig.1). The primary surface is comprised of the sliding pad, made of filled PTFE and partially recessed into the slider, and a mating sheet of stainless steel, 2 mm thick, lining the concave surface of the sliding plate. The secondary surface is comprised of the rotation pad, a lubricated low-friction material, embedded into the rotation plate and a mating sheet of stainless steel lining the convex surface of the slider. The sliding plate, the rotation plate and the slider are made of carbon steel.

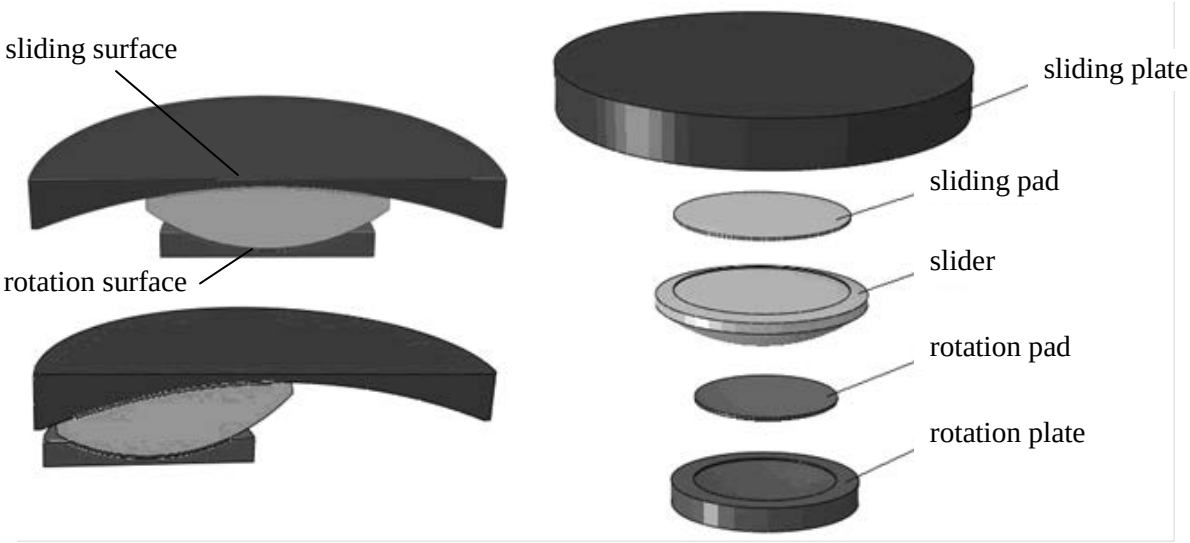

Fig. 1 – Operation principle and nomenclature of CSS [20]

2.2 Finite element model

A three-dimensional model of the bearing was created in the commercial code ABAQUS v. 6.10 (Dassault Systèmes Simulia Corp., Providence, RI) and subdivided in a mesh of three dimensional finite elements. Either linear thermal-mechanical coupled hexaedrical or wedge elements, type C3D8T and C3D6T respectively, with four degrees of freedom (the three displacement components and the temperature) at each node, were used. Mechanical and thermal properties were assigned to the materials in accordance with Table 1.

Table 1 – Material properties [8]

material	Modulus (MPa)	Possion ratio (-)	conductivity (mW/(mm K))	specific heat (J/(kg K))
carbon steel	$2.09 \cdot 10^5$	0.30	53.7	$4.9 \cdot 10^5$
stainless steel	$1.96 \cdot 10^5$	0.30	16.0	$5.0 \cdot 10^5$
sliding pad	$8.00 \cdot 10^2$	0.45	0.65	$1.1 \cdot 10^6$
rotation pad	$2.80 \cdot 10^3$	0.45	0.25	$1.7 \cdot 10^6$

Heat generation at the primary surface was simulated by introducing a heat source spread over the whole area of the sliding pad of local intensity.

$$q(t) = \mu(t) \cdot p(t) \cdot V(t) \tag{1}$$

where μ is the coefficient of friction, p is the surface pressure, and V is the relative velocity of the slider respect to the mating surface. In writing Eq. (1) it was assumed that the mechanical work of the external forces to sustain the motion of the bearing is entirely converted into heat. It was also assumed that almost the totality (99%) of the heat flux is directed inwards the steel plate and only 1% inwards the sliding pad; the validity of this assumption justified by the different thermal conductivity of the relevant materials was confirmed in a thermal analysis [8].

The coefficient of friction μ was formulated as a function of the velocity of sliding V and temperature T according to the following model

$$\mu = \mu_{vel} \cdot \exp\left[-\beta \cdot (T - T_0)\right] \tag{2}$$

$$\mu_{vel} = f_{k2} - (f_{k2} - f_{k1}) \cdot \exp(-\alpha_1 \cdot V) + (f_{st} - f_{k1}) \cdot \exp(-\alpha_2 \cdot V) \cdot \frac{|\text{sign}(V) - \text{sign}(d)|}{2} \tag{3}$$

where μ_{vel} is the velocity-dependent contribution at the reference temperature T_0, f_{k1} and f_{k2} are the kinetic coefficient of friction at either low or high velocity, respectively, f_{st} is the static coefficient of friction that opposes the initiation of sliding from zero velocity, α_1 is a parameter regulating the increase in kinetic friction with velocity, d is the displacement variable, α_2 is a parameter regulating the transition from the static to the kinetic friction regime, and β represents the rate of decay of friction with temperature. To reduce the calculation burden, the variation of axial pressure on the slider, and therefore the dependence of friction on pressure, was ignored; this assumption was deemed realistic when simulating the execution of tests under constant vertical load.

The thermal boundary conditions are the heat flux at the primary surface according to Eq. (1), and the environmental temperature at the upper and lower external surfaces of the isolator. The temperature distribution within the bearing is calculated by numerical integration of the heat balance equation; the size of the time increment being self-adjusted by the software between 0.0001 seconds and 0.5 seconds in order to keep the temperature change at the sliding surface less than 5°C per increment. At each calculation step, a sub-routine adjusts the coefficient of friction based on the current nodal surface velocity and temperature according to Eq. (2) and Eq. (2), and feeds it into Eq. (1) to update the instantaneous heat flux q. The software calculates also the contact pressure and the relative velocity at the nodes of the primary surface, which are used to update the heat flux equation and the global reaction force of the isolator.

2.3 Model validation

The numerical procedure was validated based on experimental tests conducted on the CSS bearing represented in the finite element model [8]. The bearing was subjected, under the application of a constant axial load of 4,500 kN, to a reversed cyclic displacement history with period of 2.13 Hz and amplitude of either 85 mm (Test1) or 170 mm(Test2). The peak velocity was 251 mm/s in Test1 and 502 mm/s in Test 2. Four complete cycles were performed at each amplitude.

The experimental protocol was reproduced in the finite element analysis, assuming the set of parameters of the friction model reported in Table 2. Plots of the friction coefficient versus the velocity at different temperature are presented in Fig.2: at constant temperature the coefficient of friction reaches a steady level at velocities above 200 mm/s [11], whereas it approximately halves when increasing the temperature from 25°C to 150°C. At the secondary surface a constant value of the coefficient of friction of 0.005 was taken, neglecting the temperature rise due to the small entity of the heat flux.

Table 2 – Parameters of the friction model [8]

parameter	f_{k1} (-)	f_{k2} (-)	f_{st} (-)	α_1 (s/mm)	α_2 (s/mm)	β (°C^{-1})
carbon steel	0.040	0.120	0.165	0.015	0.250	0.005

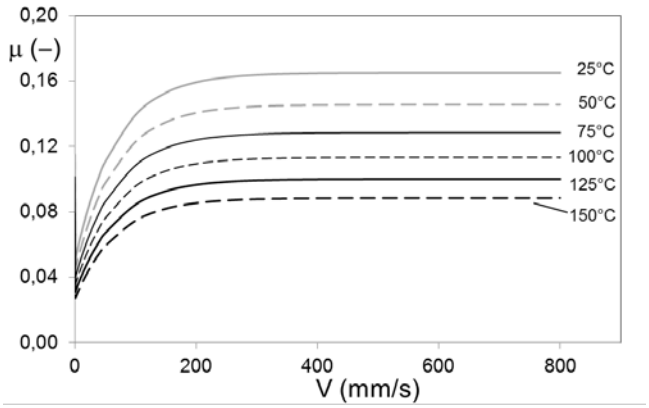

Fig. 2 – Dependence of coefficient of friction on velocity and temperature

Fig.3 compares the temperature histories measured on the back of the stainless steel liner of the primary surface (i.e. 2 mm below the actual sliding surface) at the center of the bearing (TC1) and 260 mm apart (TC5) where the peak temperature is recorded, with the relevant histories provided from the analyses.

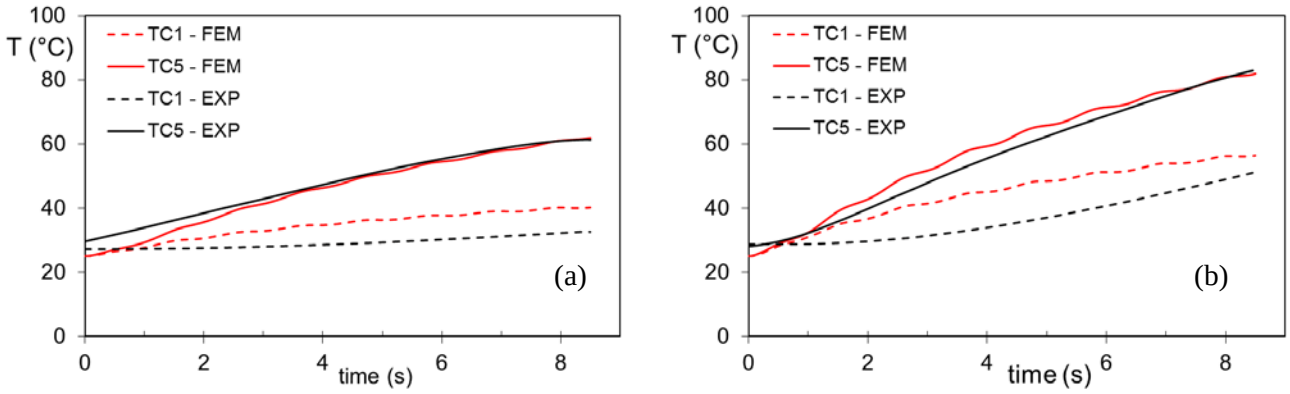

Fig. 3 – Temperature histories on the back of the stainless steel surface in either Test1, A = 85 mm (a) and Test2, A = 170 mm (b). Finite element analyses (FEM) vs. thermocouple measurement (EXP) [20]

The hysteretic force–displacement loops calculated by the finite element model matched the experimental curves (Fig.4). By accounting for the temperature-dependent friction formulation, the numerical analyses were able to replicate the decrease of the effective stiffness and the Energy Dissipated per Cycle (Fig.4), with a maximum deviation of about 3% for the stiffness and 4% for the EDC in Test 2, and of 4.4% for the stiffness and about 7% for the EDC in Test 1.

In conclusion, the agreement between the numerical predictions and the experimental histories of both mechanical and thermal variables measured in the laboratory tests was good, proving the accuracy of the numerical procedure.

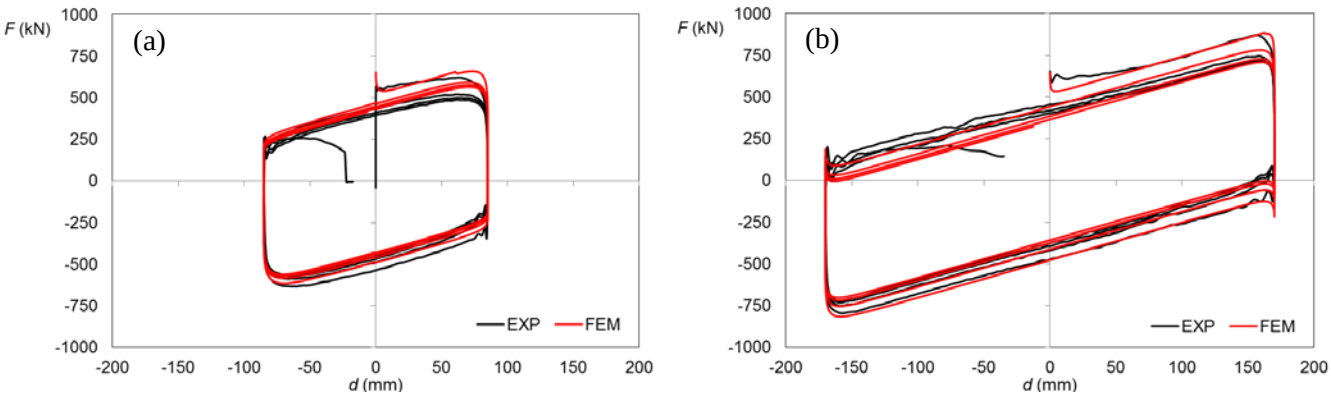

Fig. 4 – Hysteretic load – displacement curves in either Test1, A = 85 mm (a) and Test2, A = 170 mm [20]

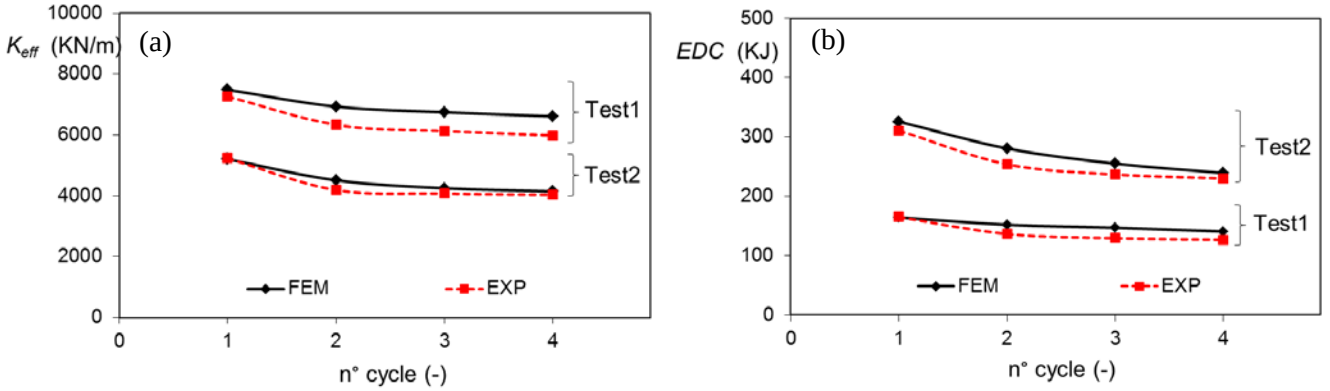

Fig. 5 – Hysteretic load – displacement curves in either Test1, A = 85 mm (a) and Test2, A = 170 mm [20]

3. Bidirectional motion analysis

3.1 Displacement histories

Numerical analyses were conducted under either unidirectional or multidirectional trajectories formulated though the displacement components $d_X(t)$ and $d_Y(t)$ in the horizontal x and y directions [20]:

$$\begin{cases} d_X(t) = A_{X,0} + A_X \cos(n_X \cdot \omega \cdot t) \\ d_Y(t) = A_{Y,0} + A_Y \operatorname{sen}(n_Y \cdot \omega \cdot t) \end{cases} \quad (4)$$

A_X and A_Y denote the displacement amplitude in either direction, $A_{X,0}$ and $A_{Y,0}$ are the initial off-sets, n_X and n_Y are integer (0, 1 or 2), t is the time variable, $\omega = 2\pi/T$ is the circular frequency, and T = 2.13 s is the natural period of the isolator.

Different displacement orbits were simulated by varying the parameters in accordance with the parameters established in Table 3. The bearing was subjected to an axial load of N = 4,500 kN and four complete cycles

were performed in each analysis, for a duration of 8.52 seconds. The unidirectional orbit reproduces the typical displacement trajectory developed in laboratory testing according to the standards. The circular and 8-shaped orbits develop bidirectional trajectories with maximum displacement in the x and y axes equal to the extreme displacement of the unidirectional analysis, and the same is for the elliptical orbit but for the displacement amplitude in the y direction which is set to 0.5 times A_x.

Table 3 – Displacement orbit parameters

orbit ID	A_X (mm)	A_Y (mm)	$A_{X,0}$ (mm)	$A_{Y,0}$ (mm)	n_X (-)	n_Y (-)
unidirectional	170	0	0	0	1	0
circular	170	170	0	0	1	1
elliptical	170	85	0	0	1	1
8-shaped	170	170	0	0	1	2

During the analysis the ambient temperature at the upper and lower external surfaces of the isolator was kept constant at 25°C, simulating the effect of a massive structure (e.g. a large building or a bulk testing frame) housing the bearing. Conductivity heat transmission was allowed at the primary and secondary sliding surfaces of the bearing, while the lateral surfaces of the isolator were modelled as adiabatic (a realistic assumption for short time duration events).

3.2 Results

Fig.6 illustrates the response of the CSS unit under the different displacement orbits (only one cycle for each orbit), in terms of resisting force–displacement loops along the x and y axis (Fig.6a), force locus in the x-y plane (Fig.6b), and direction and magnitude of the resisting force (shear force) vector at given points of the displacement orbit (Fig.6c). Bidirectional trajectories lead to highly nonlinear hysteretic loops, different from the classical bilinear loops typically produced in unidirectional tests. Another effect of the multidirectional orbits is that lower peak forces are produced at the extreme displacements respect to the unidirectional orbit (Fig. 7). Here the change of the level of resisting force at a given displacement of the bearing in two subsequent cycles is an effect of the frictional heating on the coefficient of friction.

Fig.8 presents the histories of the local peak temperature and of the average surface temperature on the sliding pad. The temperature continuously increases during the four cycles of motion, and is higher for multidirectional orbits than unidirectional ones: after 8.52 seconds the gap between the 8-shaped orbit and the unidirectional orbit temperature is 57°C for the average value and 47°C for the peak value.

The multidirectional orbits increase the energy dissipation (Fig.9), but in spite of the relevant larger temperature increase associated to these orbits, the decay in EDC with respect to the first cycle does not seem to have an important dependence on the path of motion.

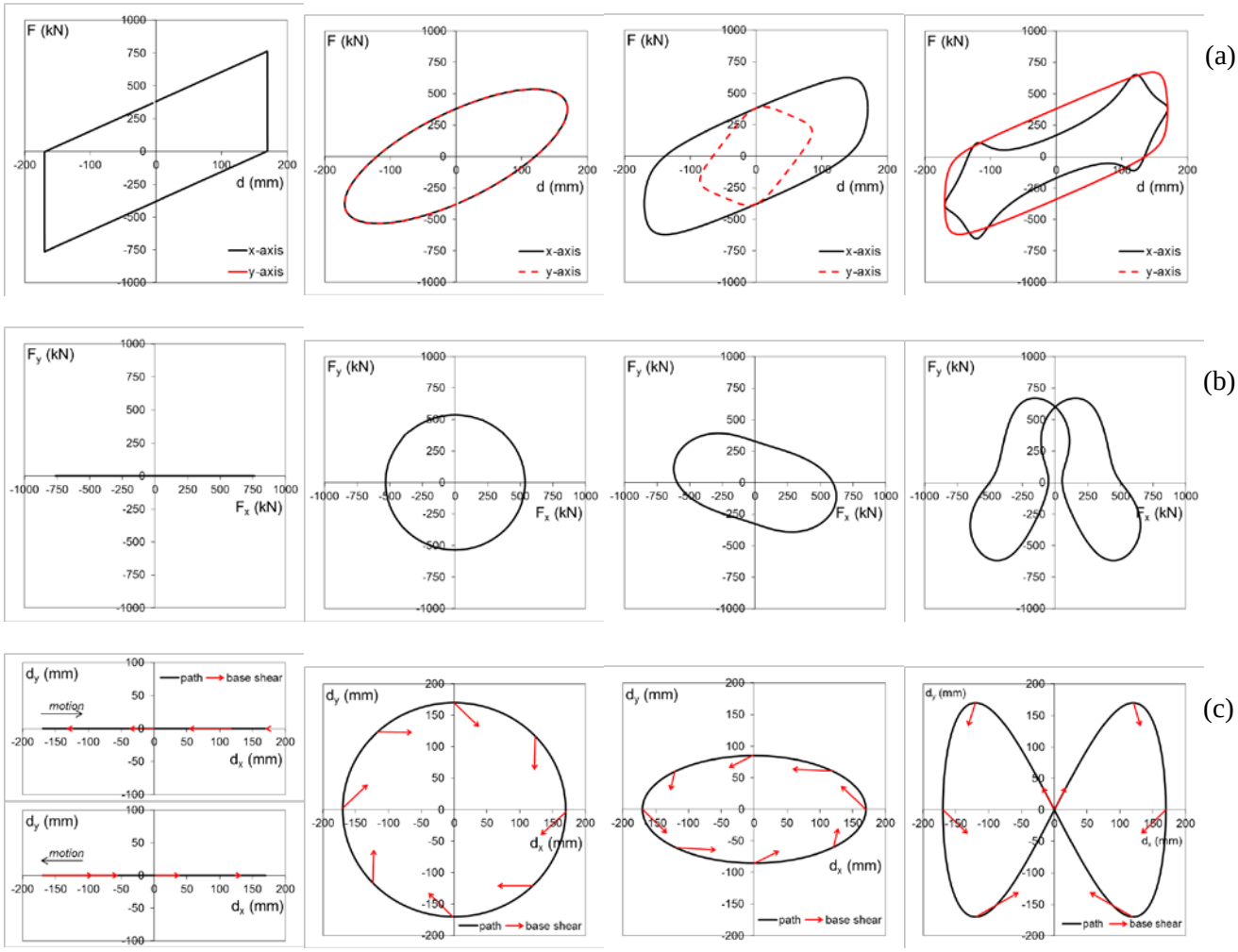

unidirectional	circular	elliptical	8-shaped

Fig. 6 – CSS responses under different orbits: unidirectional

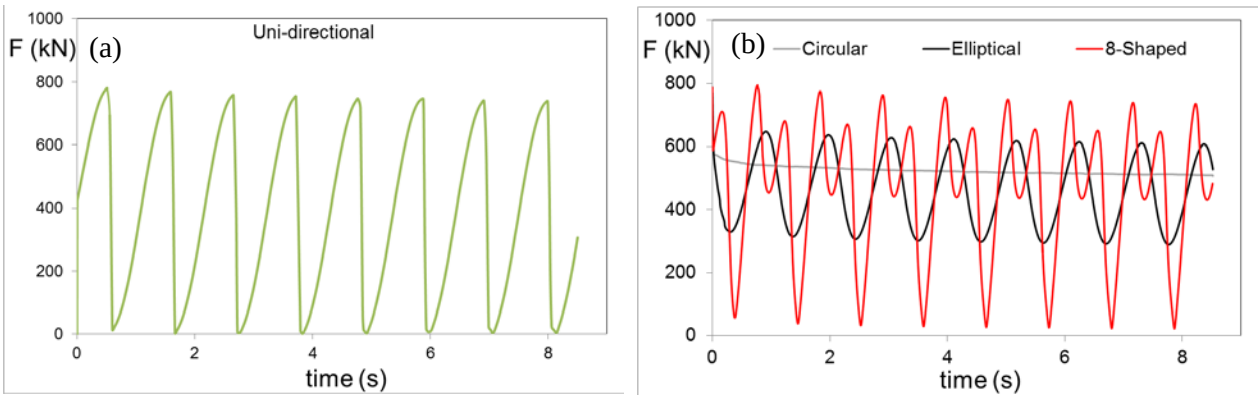

Fig. 7 – Bearing resisting force histories of unidirectional (a) and multidirectional orbits (b)

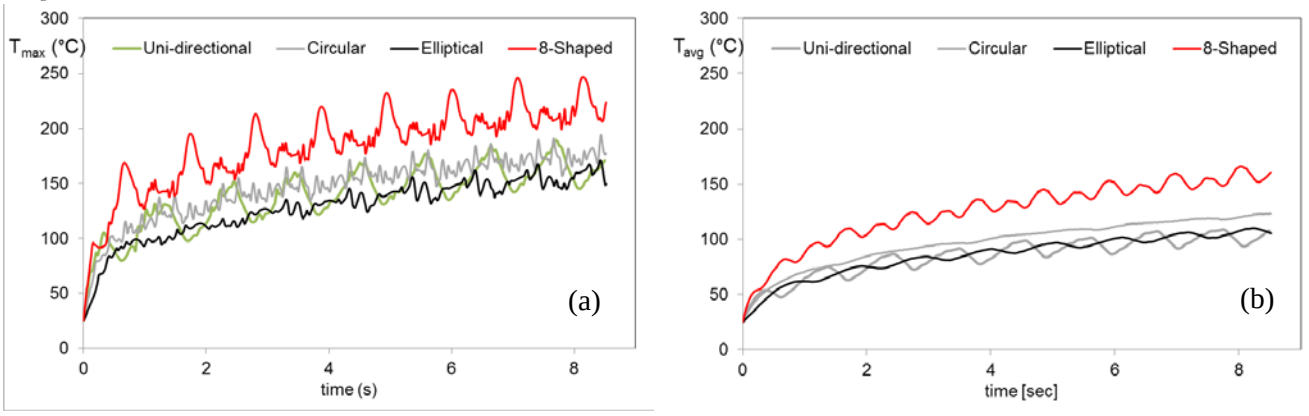

Fig. 8 – Temperature histories on the pad surface: maximum local (a) and average surface temperature (b)

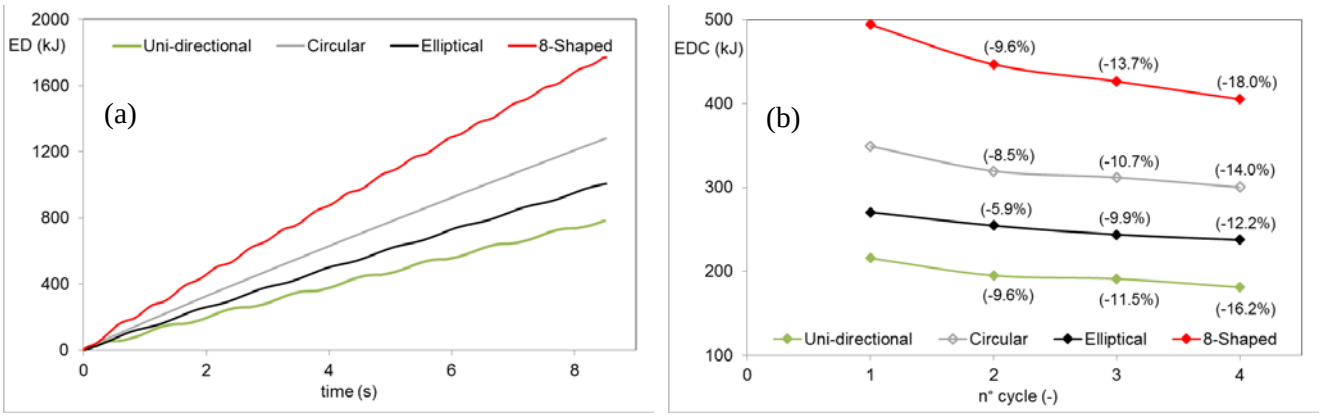

Fig. 9 – Energy Dissipated (ED): time histories (a) and dissipation per cycle (b). Between brackets: relative decrease of EDC with respect to the first cycle [20]

4. Discussion

The response of the Curved Surface Slider to different displacement orbits, characterized by the same displacement amplitude in either the x and y direction and same fundamental period, was investigated by means of numerical analysis. It must be noted that though the velocity profiles of the orbits are different, the relevant velocity fluctuations are in the range of steady coefficient of friction shown in Fig.2 and therefore the velocity effect on the friction force is deemed to be not significant. However, the velocity of sliding is expected to have a substantial effect on the energy dissipation and the frictional heating.

4.1 Resisting force

The resisting force of the CSS at a given displacement is given by the composition of two contributions [1]: the "pendulum" or restoring force, which is proportional to the local slope of the curved surface at the contact point between the slider and the sliding plate and is always acting towards the center of the bearing, and the "frictional" force which is proportional to the sliding velocity through the coefficient of friction and is acting in the direction opposite to the instantaneous velocity vector. Hence at a given position of the bearing the restoring force has always the same magnitude and direction whichever the path followed by the slider to approach the position, whereas the frictional force is tangent to the trajectory of the slider and its magnitude depends on the current velocity.

Consider first the displacement at (170;0) mm point. Because the various orbits approach this point along different paths, the frictional force components in the x and y directions are different. The largest value of the resisting force occurs when the slider approaches the position from the direction pointing towards the center of the bearing, as both the pendulum and the friction force are parallel to each other and sum up as in the unidirectional motion. The largest resisting force (800 kN) is developed in the unidirectional orbit and the smallest (539 kN) in the circular orbit, because the restoring force and the friction force are perpendicular to each other.

As a second example of path-dependent effect, consider the displacement at (0;0) mm point in the 8-shaped orbit. At this point, the slope of the sliding surface is null and the resisting force depends on the frictional term only. Fig. 6(c) shows that the forces depart in two different directions depending on the direction this point is approached from.

As a third example, in the circular orbit the relative movement between the slider and the sliding plate occurs at constant speed along a constant level trajectory on the curved surface, and therefore the intensity of the resisting force is constant whichever the position on the orbit.

4.2 Surface temperature

The path of motion affects the temperature growth at the sliding surface in two ways. First, the heat flux generated by friction is proportional to the sliding speed. Second, as the heat source coincides with the area of the pad surface, at any position of the mating steel surface through which heat flows away from the pad the heat flux history is periodic and intermittent; orbit paths characterized by longer times between intermittent heating at the same position of the mating surface allow larger cooling and limit the temperature increase.

The temperature histories reported in Fig.8 point to the importance of these two contributions (i) though the average speed of the circular orbit is higher than the speed of the elliptical and of the unidirectional orbits (501.2 mm/s respect to either 386.6 mm/s and 319.2 mm/s, respectively), the temperature rises associated to the three orbits are quite similar due to the longer period of intermittent heating in the circular path; (ii) in case of the 8-shaped orbit, owing to the very high speed (the average velocity over one cycle is 752.6 mm/s), the large amount of energy produces extreme temperature rises, and local peak temperature as high as 246.6°C and average temperature as high as 166°C were calculated, compared to respectively 189.7°C and 108.9°C for the unidirectional orbit. If one considers that the practical temperature limits of current sliding materials are about 110°C for UHMWPE and 260°C for PTFE, the temperature increase produced in unidirectional tests can underestimate the actual growth occurring under the chaotic multi-directional motion of a real earthquake, hence leading to a not conservative evaluation of the resistance of the pad with regards to the effects of frictional heating. It is also interesting to remark the gap between the average temperature of the pad surface, and the peak values obtained at the most stressed areas of the surface [8]. Relying on the average temperature rise of the surface can lead to underestimate even considerably the extreme temperatures experienced by the material, and the potential non uniform wear of the pad.

It must be also noted that in the analyses carried out within the study, the most adverse condition wherein the amplitude of the motion is less than the radius of the sliding pad was considered; however in practical situations the amplitude of motion is in general larger than the radius of the pad, hence allowing longer time for intermittent heating of the mating steel surface especially in case of multidirectional orbits [7].

4.3 Energy dissipation

The amount of energy dissipated by the Curved Surface Slider is given by the product of the frictional force of the bearing and the sliding speed, and therefore is higher for multidirectional orbits, Fig.9(a). An estimation of the damping capability of the bearing based on unidirectional tests can be overconservative with respect to orbits characterized by very high speeds. The dissipation capability during sustained displacement histories is also affected by the temperature rise, being velocity the same: after three cycles of motion the decrease of EDC respect to the first cycle ranges from 10% for the elliptical orbit to 11.5% for the unidirectional orbit and to 13.7% for the 8-shaped orbit, while after four cycles the decrease ranges from 12.2% to 18, Figure 9(b).

4. Conclusions

The response of a Curved Surface Slider unit to either unidirectional or multidirectional displacement-controlled orbits characterized by same displacement amplitude along the reference axes and same fundamental period has been investigated in numerical analyses.

The main novelty of the study is the focus on the effects of frictional heating by using a thermal-mechanical finite element formulation and a temperature-dependent friction model, which permit to predict the temperature rise inside the bearing and to account for its effects on the mechanical response of the device.

The main results can be summarized in the next points:

(1) lower peak forces are produced under multidirectional respect to unidirectional trajectories; the force-displacement hysteretic loops generated in multidirectional motion can be largely nonlinear, and very different in shape from the bilinear loops produced in the unidirectional motion;

(2) the level of damping is orbit-specific; the amount of energy dissipated in unidirectional motion can considerably underestimate the actual dissipation capability of the bearing under general trajectories;

(3) unidirectional tests do not replicate the temperature increase that may occur during a real earthquake characterized by a chaotic multidirectional motion, being displacement amplitude and fundamental period of the isolator unchanged.

A practical implication is that the unidirectional tests prescribed in the current standards on antiseismic devices [4-6], though over conservative with respect to the determination of the resisting force of the bearing, can be not suitable to assess the lining materials of the sliding surfaces with respect to their temperature-dependent characteristics. The Authors argue that the result presented in the paper may represent a basis for discussion in the future revision of the standards.

5. Acknowledgements

This work has been partially funded by the ReLUIS (Laboratories University Network of Seismic Engineering) Consortium within the ReLUIS/DPC 2014–2018 research program (Research line: Seismic Isolation & Energy Dissipation).

6. References

[1] Zayas VA, Low SS, Mahin SA (1987): The FPS earthquake protection system: experimental report. *Report UCB/EERC-87/01*, Earthquake Engineering Research Center, Berkeley, USA.

[2] Zayas VA, Low SS, Mahin SA (1990): A simple pendulum technique for achieving seismic isolation. *Earthquake Spectra*, **6** (2), 317–333. doi:10.1193/1.1585573.

[3] Mokha AS, Constantinou MC, Reinhhorn AM (1991): Experimental study of friction-pendulum isolation system. *Journal of Structural Engineering*, **117** (4), 1201–1217. doi:10.1061/(ASCE)0733-9445(1991)117:4(1201).

[4] EN 15129 (2009): Antiseismic Devices. CEN Comité Européen de Normalisation, Brussels, B.

[5] ASCE/SEI 7-10 (201): *Minimum Design Loads for Buildings and Other Structures*. American Society of Civil Engineers ASCE, Reston, USA.

[6] AASHTO (2014): *Guide Specifications for Seismic Isolation Design*. American Association of State Highway and Transportation Officials, Washington DC, USA.

[7] Constantinou MC, Whittaker AS, Kalpakidis Y, Fenz DM, Warn GP (2007): Performance of seismic isolation hardware under service and seismic loading. *Report MCEER-07-0012*, National Center for Earthquake Engineering Research, Buffalo, USA.

[8] Quaglini V, Bocciarelli M, Gandelli E, Dubini P (2014): Numerical assessment of frictional heating in sliding bearings for seismic isolation. *Journal of Earthquake Engineering*, **18** (8), 1198-1216. doi: 10.1080/13632469.2014.924890.

[9] Dolce M, Cardone D, Croatto F (2005): Frictional behavior of steel-PTFE interfaces for seismic isolation. *Bulletin of Earthquake Engineering*, **3** (2), 75-99. doi:10.1007/s10518-005-0187-9.

[10] Braun C (2009): The Sliding Isolation Pendulum – an improved recentring bridge bearing. *Steel Constructions*, **2** (3), 203-206.

[11] Quaglini V, Dubini P, Poggi C (2012): Experimental assessment of sliding materials for seismic isolation systems. *Bulletin of Earthquake Engineering*, **10** (2), 717–740. doi:10.1007/s10518-011-9308-9.

[12] Wolff E (1999): Frictional heating in sliding bearings and an experimental study of high friction materials. PhD Thesis, State University of New York, Buffalo, USA.

[13] Mosqueda G, Whittaker AS, Fenves GL (2004: Characterization and modeling of friction pendulum bearings subjected to multiple components of excitation. *Journal of Structural Engineering*, **130** (3), 433-442. doi:10.1061/(ASCE)0733-9445(2004)130:3(433).

[14] Clarke CSJ, Buchanan R, Efthymiou M (2005): Structural platform solution for seismic arctic environments – Sakhalin II offshore facilities. *Proceedings of Offshore Technology Conference*, Houston, USA.

[15] Drozdov YN, Nadein VA, Puchkov VN, Puchkov MV (2008): Heat state of pendulum sliding bearings under seismic effects. *Journal of Friction and Wear*, **29** (4), 265-270.

[16] Kumar M, Whittaker AS, Constantinou MC (2015): Characterizing friction in sliding isolation bearings. *Earthquake Engineering and Structural Dynamics*, **44** (9), 1409-1425. doi:10.1002/eqe.2524.

[17] Becker TC, Mahin SA (2012): Experimental and analytical study of the bi-directional Behavior of the Triple Friction Pendulum Isolator. *Earthquake Engineering and Structural Dynamics*, **41** (3), 355-373. doi:10.1002/eqe.1133

[18] Lomiento G, Bonessio N, Benzoni G (2013): Friction model for sliding bearings under seismic excitation. *Journal of Earthquake Engineering*, **17** (8), 1162-1191. doi:10.1080/13632469.2013.814611.

[19] Furinghetti M, Casarotti C, Pavese A (2014): Bi-directional experimental response of full scale DCSS devices. *2nd ECEES European Conference on Earthquake Engineering and Seismology*, Istanbul, TR.

[20] Quaglini V, Gandelli E, Bocciarelli M, Dubini P (2015): Numerical investigation of frictional heating in Curved Surface Sliders. *14th World Conference on Seismic Isolation, Energy Dissipation and Active Vibration Control of Structures*, San Diego, USA.